



EDGEWOOD CHEMICAL BIOLOGICAL CENTER

U.S. ARMY RESEARCH, DEVELOPMENT AND ENGINEERING COMMAND
Aberdeen Proving Ground, MD 21010-5424

ECBC-TR-1296

PHYSICS-BASED MODELING OF PERMEATION: SIMULATION OF LOW-VOLATILITY AGENT PERMEATION AND AEROSOL VAPOR LIQUID ASSESSMENT GROUP EXPERIMENTS

Brent A. Mantooth
Terrence G. D'Onofrio

RESEARCH AND TECHNOLOGY DIRECTORATE

Mark J. Varady

OPTIMETRICS, INC., A DCS COMPANY
Abingdon, MD 21009-1283

June 2015

Approved for public release; distribution is unlimited.



Disclaimer

The findings in this report are not to be construed as an official Department of the Army position unless so designated by other authorizing documents.

REPORT DOCUMENTATION PAGE				Form Approved OMB No. 0704-0188	
Public reporting burden for this collection of information is estimated to average 1 h per response, including the time for reviewing instructions, searching existing data sources, gathering and maintaining the data needed, and completing and reviewing this collection of information. Send comments regarding this burden estimate or any other aspect of this collection of information, including suggestions for reducing this burden to Department of Defense, Washington Headquarters Services, Directorate for Information Operations and Reports (0704-0188), 1215 Jefferson Davis Highway, Suite 1204, Arlington, VA 22202-4302. Respondents should be aware that notwithstanding any other provision of law, no person shall be subject to any penalty for failing to comply with a collection of information if it does not display a currently valid OMB control number. PLEASE DO NOT RETURN YOUR FORM TO THE ABOVE ADDRESS.					
1. REPORT DATE (DD-MM-YYYY) XX-06-2015		2. REPORT TYPE Final		3. DATES COVERED (From - To) Jan 2014 – Sep 2014	
4. TITLE AND SUBTITLE Physics-Based Modeling of Permeation: Simulation of Low-Volatility Agent Permeation and Aerosol Vapor Liquid Assessment Group Experiments				5a. CONTRACT NUMBER	
				5b. GRANT NUMBER	
				5c. PROGRAM ELEMENT NUMBER	
6. AUTHOR(S) Mantooth, Brent A.; D'Onofrio, Terrence G. (ECBC); Varady, Mark J. (OptiMetrics)				5d. PROJECT NUMBER HDTRA1411111	
				5e. TASK NUMBER	
				5f. WORK UNIT NUMBER	
7. PERFORMING ORGANIZATION NAME(S) AND ADDRESS(ES) Director, ECBC, ATTN: RDCB-DRP-D, APG, MD 21010-5424 OptiMetrics, Inc., a DCS Company, 100 Walter Ward Blvd., Suite 100, Abingdon, MD 21009-1283				8. PERFORMING ORGANIZATION REPORT NUMBER ECBC-TR-1296	
9. SPONSORING / MONITORING AGENCY NAME(S) AND ADDRESS(ES) Deputy Under Secretary of the Army for Test and Evaluation 102 Army Pentagon Washington, DC 20310-0102				10. SPONSOR/MONITOR'S ACRONYM(S) DUSA TE	
				11. SPONSOR/MONITOR'S REPORT NUMBER(S)	
12. DISTRIBUTION / AVAILABILITY STATEMENT Approved for public release; distribution is unlimited.					
13. SUPPLEMENTARY NOTES					
14. ABSTRACT: Physics-based models were developed to predict agent permeation through test material swatches in the low-volatility agent permeation (LVAP) and Aerosol Vapor Liquid Assessment Group (AVLAG) cell tests. The model tracks the transport and distribution of agent in the liquid, material swatch, and collection media (sampler or air stream). For the LVAP tests, model predictions were compared to experimental results and showed good agreement. The model predictions provided additional insight into the physical processes occurring during permeation and were used to study hypothetical test materials with desired properties. Comparing model results for LVAP and AVLAG tests revealed the physical reasons for the differences in permeation rates for low vapor pressure agents such as VX. The LVAP model was shown to provide a reasonable worst-case scenario for permeation into skin in a real-world scenario because good contact is maintained between the test material and sampler. A simple model was developed to investigate the effect of imperfect contact between the test material and sampler on the permeation rate. Suggestions were also made for further model development efforts in the area of agent permeation through materials.					
15. SUBJECT TERMS <div style="display: flex; justify-content: space-between;"> <div>Low-volatility agent permeation (LVAP) Aerosol vapor liquid assessment group (AVLAG)</div> <div>Permeation testing Physics-based modeling</div> <div>Protective equipment Contact test</div> <div>VX</div> </div>					
16. SECURITY CLASSIFICATION OF:			17. LIMITATION OF ABSTRACT	18. NUMBER OF PAGES	19a. NAME OF RESPONSIBLE PERSON
a. REPORT	b. ABSTRACT	c. THIS PAGE			19b. TELEPHONE NUMBER (include area code)
U	U	U	UU	36	Renu B. Rastogi (410) 436-7545

Blank

PREFACE

The work described in this report was authorized under Deputy Under Secretary of the Army for Test and Evaluation (DUSA TE) project number HDTRA1411111. The work was started in January 2014 and completed in September 2014.

The use of either trade or manufacturers' names in this report does not constitute an official endorsement of any commercial products. This report may not be cited for purposes of advertisement.

This report has been approved for public release.

Acknowledgments

A program cannot be successfully completed without the contributions of a good team of people. The authors thank the following individuals for their hard work and assistance with the execution of this technical program:

- Patrick Riley (Leidos, Inc.; Abingdon, MD) for running the dynamic contact angle experiments
- Kayla Cooley (OptiMetrics, Inc.; Abingdon, MD) for scanning electron microscopy of samples
- Megan Holste (DUSA TE; Washington, DC) for funding support

Blank

CONTENTS

1.	INTRODUCTION	1
2.	MODEL DEVELOPMENT AND IMPLEMENTATION	2
2.1	LVAP Model Equations	3
2.2	AVLAG Model Equations.....	4
2.3	Model Parameter Determination	4
2.3.1	Transport Properties for VX in DVB.....	5
2.3.2	Transport Properties for VX in Latex	6
2.3.3	Transport Properties for VX in Neoprene.....	6
2.3.4	Transport Properties for VX in Air.....	7
2.4	Model Implementation	8
3.	LVAP MODEL ASSESSMENT AND SENSITIVITY ANALYSIS.....	8
3.1	Comparison of LVAP Model Predictions to Experimental Results	8
3.2	Sensitivity Analysis.....	10
3.2.1	Effect of Material Thickness on Permeation	10
3.2.2	Effect of Transport Properties on Permeation	11
4.	COMPARISON OF LVAP AND AVLAG TEST METHODOLOGIES	13
5.	COMPARISON OF LVAP PERMEATION RESULTS TO IDEAL MODEL OF SKIN UPTAKE	15
6.	EFFECT OF VAPOR PRESSURE ON PERMEATION RATE IN AVLAG CELL.....	16
7.	EFFECTS OF IMPERFECT MATERIAL–SAMPLER CONTACT	18
8.	CONCLUSIONS AND SUGGESTIONS FOR FUTURE WORK	19
	LITERATURE CITED	21
	ACRONYMS AND ABBREVIATIONS	23

FIGURES

1.	Schematics of (a) LVAP and (b) AVLAG experiments showing permeation of agent through test material. The permeated agent is absorbed by the contact sampler in the LVAP test and swept into a vapor sampler for quantification in the AVLAG test.	2
2.	(a) Time evolution of VX droplet volume sitting on top of DVB pad, measured with DCA. (b) Image of the microsphere structure of the DVB pad obtained with a scanning electron microscope.	5
3.	Experimental determination of (a) saturation concentration and (b) diffusivity of <i>n</i> -alkanes in neoprene from Harogoppad et al. ^{13,14} Also shown are power law fits to molecular weight, used to extrapolate and obtain approximate values for VX in neoprene, which are indicated by the red stars.	7
4.	Model-predicted time evolution of VX mass in all phases throughout a simulated 24 h LVAP test for (left) latex and (right) neoprene. The blue line indicates the mass in the liquid phase, green line indicates the mass of VX in the material, and red line indicates the mass in the contact sampler. The vertical green arrows denote the breakthrough time. Also shown are the experimental results for total VX mass permeated for both latex and neoprene, obtained during LVAP verification testing. ¹²	8
5.	A movie clip showing the concentration profile evolution for VX. Press the play button to activate.....	9
6.	Model-predicted VX mass permeated through (1a) latex and (1b) neoprene as a function of time for nominal thicknesses and for +20 and –20% thicknesses. Also shown are the differences in permeated mass between the $\pm 20\%$ thickness extremes for both (2a) latex and (2b) neoprene.	10
7.	Model-predicted time evolution of agent mass in material and sampler throughout a simulated 24 h LVAP test for hypothetical porous material.	11
8.	Model-predicted time evolution of agent mass in material and sampler throughout a simulated 24 h LVAP test for a hypothetical low-solubility material.	12
9.	Model-predicted time evolution of agent mass in material and sampler throughout a simulated 24 h LVAP test for hypothetical barrier material.....	13
10.	Comparison of VX mass permeated through (a) latex and (b) neoprene using the LVAP and AVLAG methods. Also shown are the results for a modified AVLAG method where the droplets were spread into a thin liquid film as opposed to being sessile.	13
11.	Contours of VX concentration during a simulated AVLAG cell test for VX permeation through neoprene.	14
12.	Mass of VX permeated through (a) latex and (b) neoprene in simulated LVAP tests using DVB and skin as samplers.	16
13.	Comparison of predicted permeation results from simulated standard AVLAG cell test using hypothetical agents with vapor pressures of 2 and 20 Pa for (a) latex and (b) neoprene.....	17
14.	Schematic of model used to simulate imperfect contact between material and sampler during an LVAP test. A sinusoidal function is used to represent the surface of the material in contact with the sampler, and the distance (Δ) between the material and sampler controls the local contact area (A_c).	19
15.	Mass of VX permeated through latex in an LVAP experiment with varying degrees of contact between the latex and DVB sampler.....	19

TABLES

1.	Calculated Transport Parameters of Diffusivity and Saturation for Materials Used in this Report.....	5
2.	Summary of Experimental Conditions and Results for Two Different LVAP Tests for VX Permeation through Latex	6
3.	Summary of Model-Predicted VX Permeation for Different Experimental Configurations	14

Blank

PHYSICS-BASED MODELING OF PERMEATION: SIMULATION OF LOW-VOLATILITY AGENT PERMEATION AND AEROSOL VAPOR LIQUID ASSESSMENT GROUP EXPERIMENTS

1. INTRODUCTION

When a liquid-phase agent is deposited onto a material, the chemical species can sorb into the material and eventually emerge on the opposite side. This is known as *permeation*. Protective equipment is specifically designed to prevent this process. To ensure that protective equipment performs according to specifications, tests are conducted to determine when breakthrough of agent occurs and the quantity of agent permeated over a specified time.

Several factors influence the results of a permeation test, including material composition, thickness, and stress state;^{1,2} agent–material chemical interactions; environmental conditions such as temperature and humidity; and conditions on the opposite side of the material (e.g., air or contact with skin or a skin simulant). The large number of variables involved makes exhaustive testing of a specific material–agent pair an expensive and time-consuming process. Even with a large database of permeation data, a specific “What-if?” question could be posed that falls outside the range of validity of the experimental data.

Furthermore, a single universal test that is capable of addressing permeation and breakthrough for all agent–material pairs does not exist. Several different methods are available to test agent permeation; this study discusses two of these methods. The Aerosol Vapor Liquid Assessment Group (AVLAG) cell uses an inert sweep gas to collect permeated agent at the opposite side of a contaminated material swatch.³ The test method used to measure agent permeation through materials is named for the AVLAG cell that holds the test materials. However, for low vapor pressure agents, vapor collection of analyte could not be used to accurately measure the permeated mass available for contact transfer. To address this issue, the low-volatility agent permeation (LVAP) method was developed in which a solid-phase absorbent pad is used to collect permeated agent on the opposite side of the material.⁴

In the evaluation of protective equipment for permeability, modeling is currently an under-utilized tool. A model provides valuable insight into the fundamental processes that drive permeation. Moreover, a physics-based model can be used to answer many important What-if? questions while minimizing costly testing. Models can also be used to evaluate permeation tests and offer possibilities for improvement in test methodology and design to extract the required information from the minimal necessary data.

Models also facilitate a basic understanding of the physical and chemical processes occurring during a test and can aid in interpretation of the data. For example, the AVLAG method is used to measure the vapor breakthrough, which can be appropriate for percutaneous exposures from the vapor phase, whereas the LVAP method is used to measure agent breakthrough into an absorbing material that could represent percutaneous exposures from direct contact with a contaminated material. The differences between these two test methods will result in different breakthrough mass values as a function of time because the methods have different sampling methods. Modeling can enable the interpretation of both techniques and allow mapping of what seem to be disparate results between the techniques by describing the transport phenomenon for each test method. Additionally, physics-based models can be used to predict when the total mass of agent permeated will reach a particular level, which aids in test design. Furthermore, the experimental data required to obtain the parameters for modeling can be acquired with minimal time and cost. This will enable predictive capabilities that facilitate efficient experimental designs and the capability to answer many What-if? questions.

For this report, a diffusion-based mathematical model was developed to describe the permeation of a liquid agent deposited onto a material. The following items are addressed using the models:

1. The model is used to predict the permeation of *O*-ethyl-*S*-(2-isopropylaminoethyl) methylphosphonothiolate (VX) through natural latex rubber and neoprene resulting from LVAP tests.
2. The permeation model is used to study the sensitivity of permeated mass to important parameters such as material thickness and transport properties, including the properties of the protective material and the vapor pressure of the contaminant.
3. Results from the use of AVLAG and LVAP test methodologies are predicted and compared, which can serve to quantitatively relate the results from the two different test methods.
4. Permeation into skin is estimated using the model and compared to that obtained using the LVAP method. This provides a way to correlate the LVAP results to actual skin uptake results.
5. The effect of degree of contact of a material with a sampler (e.g., skin) on the permeated mass is quantified, because perfect contact may not be encountered in real-world scenarios.

Areas for expanded modeling work in the field of permeation are featured, including multilayer and porous materials (fabrics), active materials, and optimal protective materials development.

2. MODEL DEVELOPMENT AND IMPLEMENTATION

Figure 1 shows schematics for the LVAP and AVLAG experiments. In the LVAP experiment, liquid agent is deposited onto a test swatch (i.e., material) that has been placed on an absorbent divinyl benzene (DVB) pad (sampler) to collect any permeated agent. A weight is applied to promote contact between the material and sampler, which also causes the applied agent droplets to form a thin film. The details of the experimental procedure and data analysis can be found in *Development of a Contact Permeation Test Fixture and Method* (ECBC-TR-1141).⁴ For AVLAG experiments, no weight is applied, and the permeated contaminant is swept by the air stream to a vapor collector downstream of the agent placement.³

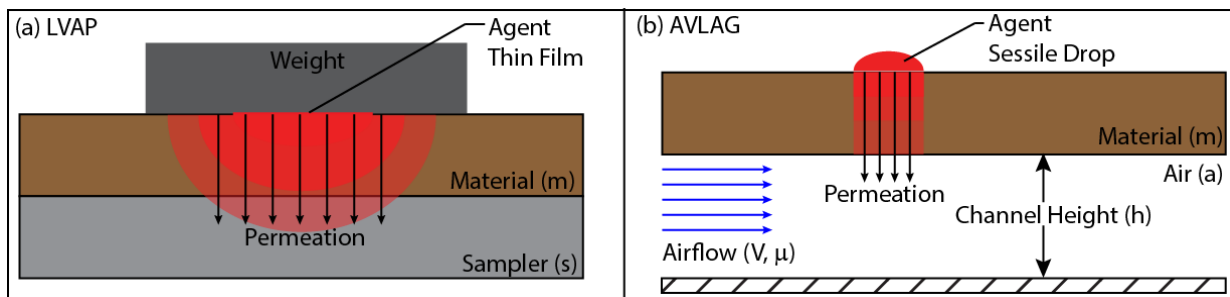


Figure 1. Schematics of (a) LVAP and (b) AVLAG experiments showing permeation of agent through test material. The permeated agent is absorbed by the contact sampler in the LVAP test and swept into a vapor collector for quantification in the AVLAG test.

2.1 LVAP Model Equations

The primary goal of the LVAP model is to predict the agent permeation through the material as a function of time. For rubbery polymeric materials it has been well-established (for over 150 years) that the concentration of agent within the material, C , is described by Fick's second law (eq 1)⁵

$$\frac{\partial C_i}{\partial t} = \nabla \cdot (D_i \nabla C_i) \quad \text{Equation 1}$$

where

D is diffusivity of agent in the material (m^2/s)

C_i is concentration of contaminant in material i (mol/m^3)

i is subscript index indicating the test material ($i = \text{m}$) or DVB sampler ($i = \text{s}$)

t is time (s)

The diffusivity, D , quantifies how fast agent molecules move through the material. At the liquid–material interface, the liquid agent is spread into a uniform thin film, and thermodynamic equilibrium is established so that the concentration of the agent is at its solubility limit in the material, $C_{\text{m,sat}}$, which is known as the saturation concentration.⁶ This is also known as the solution–diffusion transport mechanism. At the material–sampler interface, both thermodynamic equilibrium and mass conservation apply⁷

$$\frac{C_{\text{m}}}{C_{\text{s}}} = \frac{C_{\text{m,sat}}}{C_{\text{s,sat}}} \quad \text{Equation 2}$$

$$D_{\text{m}} \frac{\partial C_{\text{m}}}{\partial n} = D_{\text{s}} \frac{\partial C_{\text{s}}}{\partial n} \quad \text{Equation 3}$$

where n is the coordinate direction normal to interface (m).

The total mass of agent permeated out of the material, $m(t)$, is absorbed by the DVB sampler and is calculated by integrating the instantaneous mass of agent absorbed over the volume of the DVB pad.

$$m(t) = MW \int_{V_s} C_s(t) dV \quad \text{Equation 4}$$

where

MW is molecular weight (g/mol)

V_s is volume of sampler (m^3)

Thus, the diffusivities and the solubility limits of the agent in each the material and sampler, along with material thicknesses, are the primary factors controlling the permeation rate through the material. The diffusivity, and to a lesser degree the solubility, are temperature-dependent.⁸ Note that diffusivity and solubility are often collectively referred to as *transport properties*.

2.2 AVLAG Model Equations

To model the AVLAG cell, Fick's second law (eq 1) applies for permeation in the material in a manner identical to the LVAP model. However, the liquid is in the form of sessile droplets. Also, the opposite side of the material is exposed to flowing air. Here, a convection boundary condition is typically used to describe the agent flux, which relates the agent concentration gradient in the material at the air interface to the agent concentration in the air.⁹

$$D_m \frac{\partial C_m}{\partial n} = h_m \left(C_m \frac{C_{\text{sat},a}}{C_{\text{sat},m}} \right) \quad \text{Equation 5}$$

where

h_m is mass transfer convection coefficient (m/s)

$C_{\text{sat},a}$ is saturation concentration of agent in air (mol/m^3)

The mass transfer convection coefficient accounts for all of the details for the airflow over the material surface inside the AVLAG cell (e.g., channel geometry, flow velocity, fluid properties) so that a simple mathematical relationship can be used to compute the mass flux from a surface without needing to solve the complicated nonlinear, partial differential equations of fluid flow.⁹ Note that the value of h_m is independent of the test material under study. In this particular case, h_m is calculated using the well-established correlation for flow over a flat plate.⁹ The mass transfer coefficient used for all AVLAG simulations in this work is 7.35×10^{-4} m/s.

2.3 Model Parameter Determination

To compute the agent permeation through a given material, the diffusivities and solubility limits must be determined. These transport properties are unique to given agent-material and agent-sampler pairs and must be determined individually for each agent-material pair of interest. There are developed techniques to determine these parameters;^{10,11} however, time and budget limitations prevent the use of such methods. Instead, available data from both the literature and in-house experiments were used to approximate the transport parameters.

The two major transport properties, diffusivity and saturation, were determined for VX on latex, neoprene, DVB, and air. A summary of the calculated parameters is shown in Table 1. Subsequent sections describe the methods for obtaining these numbers.

Table 1. Calculated Transport Parameters of Diffusivity and Saturation for Materials Used in this Report

Material	Diffusivity (D_m , m^2/s)	Saturation ($C_{sat,m}$, mol/m^3)
Latex	5.0×10^{-12}	1.0×10^2
Neoprene	1.8×10^{-12}	4.0×10^2
DVB	1.3×10^{-7}	1.9×10^3
Air	4.5×10^{-6}	4.7×10^{-5}

2.3.1 Transport Properties for VX in DVB

The morphology of DVB is a collection of microspheres where the chemical nature causes strong binding with several chemicals including VX. The collection of spheres results in a porous network that can be described with an effective Fickian diffusion model. A dynamic contact angle (DCA) technique¹⁰ was used to obtain an image and measure the droplet volume on the surface of the material as a function of time. As shown in Figure 2, the time required for a 2 μ L droplet of VX to absorb into a DVB pad is approximately 6 s. This fast absorption time enables a simple approximation of the transport properties of VX in DVB. Furthermore, analysis of the rapid sorption and high capacity of the DVB pad indicates that it would not be the limiting factor in the LVAP test; therefore, inaccuracy in DVB parameters would have minimal effect on model predictions. Follow-on studies, where more resources are available, can be used to ascertain the more-detailed capillary transport–surface adsorption process occurring in DVB, if it is deemed to be important.

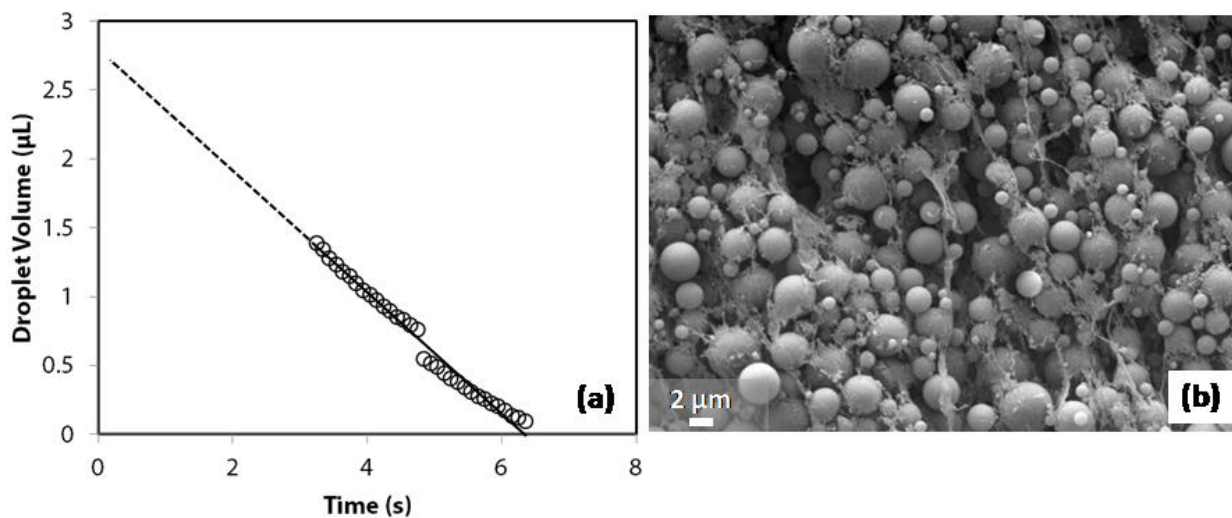


Figure 2. (a) Time evolution of VX droplet volume sitting on top of DVB pad, measured with DCA. (b) Image of the microsphere structure of the DVB pad obtained with a scanning electron microscope.

To quantitatively estimate the Fickian transport parameters from the droplet absorption test, the following approximate expression for the mass uptake of agent into the DVB, $m(t)$, was used:⁷

$$m(t) = \text{MWC}_{\text{sat},s} R_d^2 \sqrt{\frac{\pi D_s t}{2}} \quad \text{Equation 6}$$

where R_d is the radius of an applied droplet on the DVB surface (m).

The maximum capacity of VX in DVB, if no swelling occurs, would be $C_{\text{sat},c} = 3782 \text{ mol/m}^3$, which is the molar density of pure liquid VX at room temperature. However, this result would be unreasonable because no visible swelling occurs during the absorption of VX. Unfortunately, it is also impractical to saturate a DVB pad with VX because of the large quantities of chemical necessary. Multiple techniques are available to determine $C_{\text{sat},s}$, but these fall beyond the resources and scope of this program. Therefore, an educated estimate of the transport properties of VX in DVB was made to build a predictive model. Additionally, because the transport of VX in DVB is rapid, transport through the entire system is primarily dominated by the properties of the other materials (i.e., latex and neoprene material swatches). A reasonable value for $C_{\text{sat},s}$ is obtained by assuming about 50% of maximum capacity (i.e., pure liquid); therefore, $C_{\text{sat},s} = 1850 \text{ mol/m}^3$. Using this value in eq 6 yields the minimum value of the diffusivity, $D_s = 1.3 \times 10^{-7} \text{ m}^2/\text{s}$. These values for the transport properties of VX in DVB are used throughout this work.

2.3.2 Transport Properties for VX in Latex

Two different conditions were used in LVAP experiments performed with VX on latex, as summarized in Table 2.^{12,4} The details of these experiments are documented in *Low-Volatility Agent Permeation (LVAP) Verification and Validation Report* (ECBC-TR-1274).¹²

Table 2. Summary of Experimental Conditions and Results for Two Different LVAP Tests for VX Permeation through Latex

Experiment Time (h)	Latex Thickness (mm)	No. of VX Drops	Drop Volume (μL)	Contaminated Area (cm^2)	Mass Permeated (μg)
4	473	10	1	10	8300
24	254	6	1	6	4600

In the LVAP experiment, the liquid droplets are compressed into a thin film by the applied mass (Figure 1A), and the film thickness is expected to be independent of the number of droplets due to force balance (assuming no seepage from the edges of the applied mass). This results in a liquid film thickness of 10 μm . Using the model developed in Section 2.1 and the VX–DVB transport properties determined in Section 2.3.1, the diffusivity and solubility of VX were systematically varied to find values that produced good agreement with both experimental results. Using $C_{\text{m},\text{sat}} = 100 \text{ mol/m}^3$ and $D_m = 5 \times 10^{-12} \text{ m}^2/\text{s}$ for latex yielded a permeated mass of 5000 μg for the 6-droplet experiment (a difference of +8.7%) and 8900 μg for the 10-droplet experiment (a difference of +7.2%).

2.3.3 Transport Properties for VX in Neoprene

A different tack was taken to estimate the solubility and diffusivity of VX in neoprene in which the results of a published study were extrapolated to the case under study here. The studies performed by Harogoppad et al. measured the absorption of *n*-alkanes up to *n*-decane into various polymers, including neoprene, as a function of temperature.^{13,14} A primary output of this work was the solubility and diffusivity

of the n -alkanes in neoprene. Plotting each of these quantities as a function of the molecular weight of the alkanes studied yields clear trends that can be fit to a power law, as shown in Figure 3.

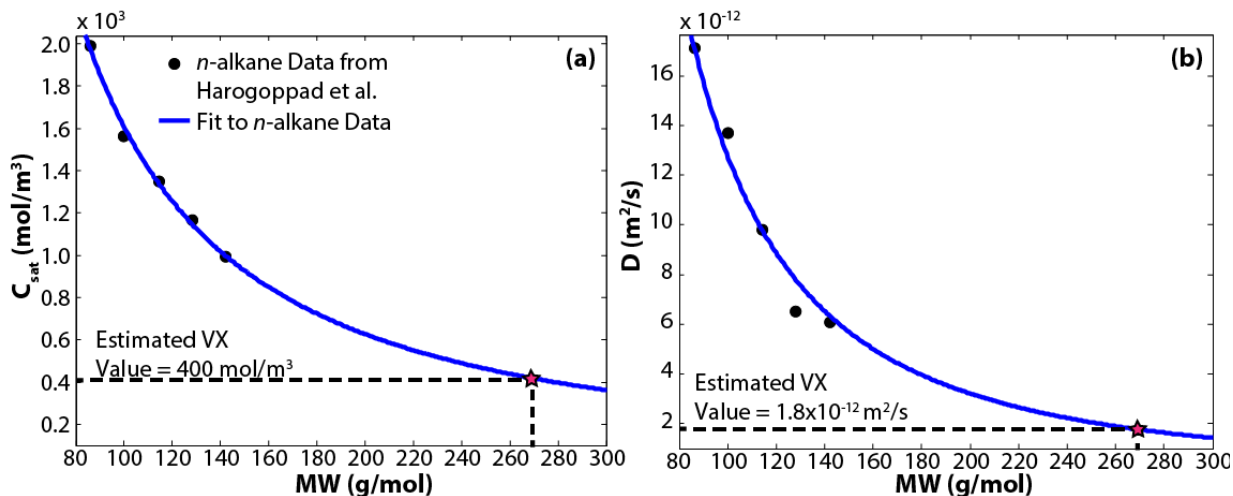


Figure 3. Experimental determination of (a) saturation concentration and (b) diffusivity of n -alkanes in neoprene from Harogoppad et al.^{13,14} Also shown are power law fits to molecular weight, used to extrapolate and obtain approximate values for VX in neoprene, which are indicated by the red stars.

The power law fit of the molecular weight of the n -alkanes to experimentally determined $C_{sat,m}$ and D_m was extrapolated to yield the values of 400 mol/m³ and 1.8×10^{-12} m²/s, respectively, for VX (MW = 267 g/mol). These values are used throughout this work to model the mass transport of VX in neoprene. Note that future efforts could be performed to experimentally determine these parameters for improved model performance.

2.3.4 Transport Properties for VX in Air

The saturation concentration (i.e., vapor pressure) and diffusivity of VX in air are required to model permeation in an AVLAG cell where the permeated VX is transferred to a stream of inert gas, which is typically sufficiently similar to air for the gas-phase molecular diffusion of VX. VX vapor pressure has been studied previously and can be given by the following Antoine equation:¹⁵

$$\ln P_{VX} = 23.72 - \frac{6154.91}{T - 60.165} \quad \text{Equation 7}$$

where

P_{VX} is vapor pressure of VX (N/m²)

T is absolute temperature (K)

The vapor pressure obtained using this equation can be converted to saturation concentration using the ideal gas law. The diffusivity of VX in air is difficult to determine experimentally, and no reliable measurements could be found in the literature. An estimate was obtained using the Wilke-Lee correlation to yield a value of 4.5×10^{-6} m²/s.¹⁶

2.4 Model Implementation

All mathematical models were implemented using the validated and benchmarked commercially available, finite-element software package COMSOL (v. 4.3b; Comsol, Inc.; Stockholm, Sweden).¹⁷ Specifically, the “Transport in Dilute Species” physics module was used to solve Fick’s second law for agent concentration and was subject to the appropriate boundary conditions as described in connection with the corresponding model development. Standard solver settings were used for all simulation runs. All two-dimensional geometries were meshed using triangular elements, and all three-dimensional geometries were meshed using tetrahedral elements. Mesh independence of results was verified for each simulation by decreasing the average element size by a factor of 2 and by checking that the computed permeated agent mass did not change by more than 5%.

3. LVAP MODEL ASSESSMENT AND SENSITIVITY ANALYSIS

3.1 Comparison of LVAP Model Predictions to Experimental Results

The model developed with the equations in Section 2.1 was used to simulate the permeation of six 1 μ L droplets of VX through latex and neoprene and collected by a DVB absorbent pad over a simulated 24 h LVAP test. The material thicknesses used were 473 and 788 μ m for latex and neoprene, respectively as specified in *Low-Volatility Agent Permeation (LVAP) Verification and Validation Report* (ECBC-TR-1274).¹² For each case, the total VX mass in the material and in the DVB sampler was computed as a function of time as shown in Figure 4, along with experimentally obtained permeated VX mass. The agreement between the model predictions at the 24 h time point and the experimental results was found to be within 10% for both latex and neoprene. A movie depicting the concentration profile evolution is shown in Figure 5.

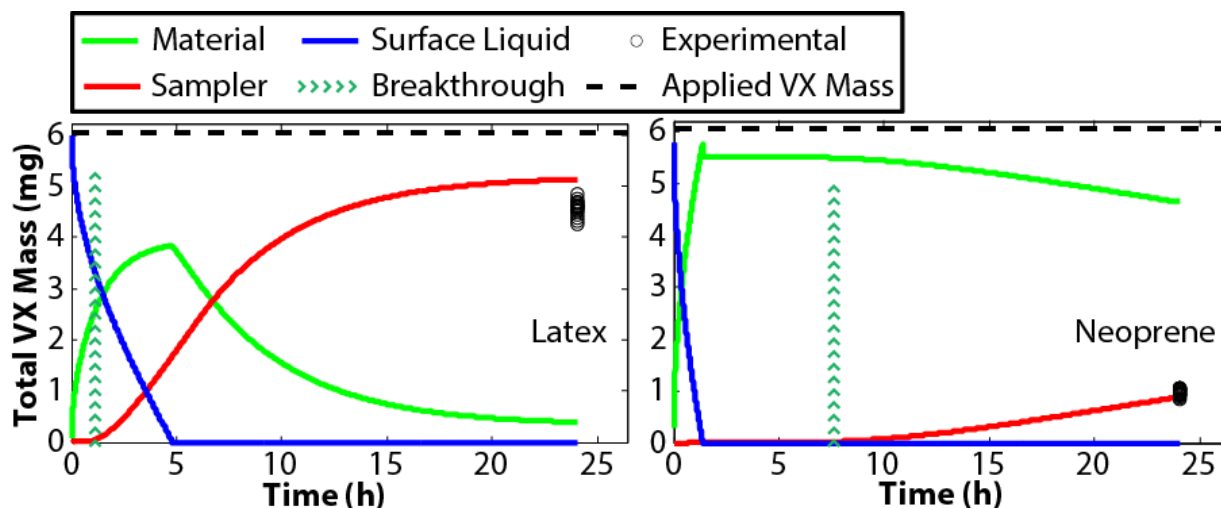


Figure 4. Model-predicted time evolution of VX mass in all phases throughout a simulated 24 h LVAP test for (left) latex and (right) neoprene. The blue line indicates the mass in the liquid phase, green line indicates the mass of VX in the material, and red line indicates the mass in the contact sampler. The vertical green arrows denote the breakthrough time. Also shown are the experimental results for total VX mass permeated for both latex and neoprene, obtained during LVAP verification testing.¹²

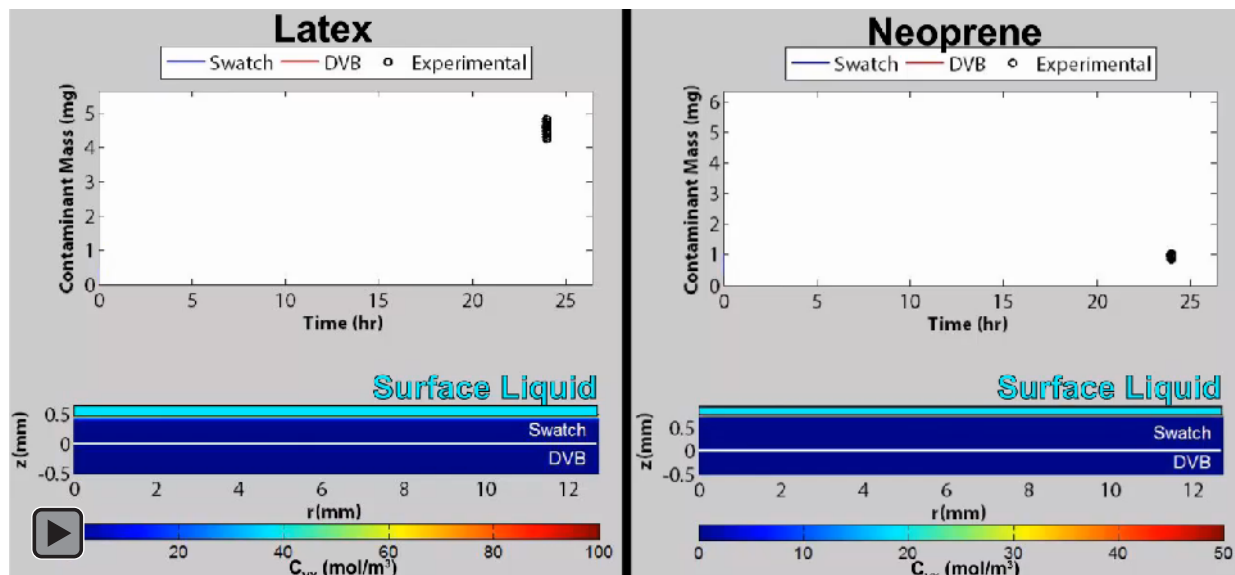


Figure 5. A movie clip showing the concentration profile evolution for VX. Press the play button to activate.

When compared with the experimental findings, the model results offered more insight into the permeation behavior of each system. As expected, VX permeated through latex faster than through neoprene, resulting in a higher total permeated mass (mass in LVAP sampler). The ability to examine the time evolution of the VX mass in both the material and sampler revealed several observations that are only available through modeling:

1. VX mass increased in the material until the surface was depleted of liquid VX, at which point VX mass began to decrease in the material. This occurred because VX has a higher affinity for the DVB sampler than for either of the materials studied ($C_{\text{sat},s} = 1850 \text{ mol/m}^3$ compared with $C_{\text{sat},m} = 100 \text{ mol/m}^3$ for latex and 400 mol/m^3 for neoprene).
2. Although VX permeated through latex faster, the liquid VX at the surface was depleted faster with neoprene. These two observations seem contradictory, but the fast surface depletion on neoprene was caused by the higher solubility limit (400 mol/m^3 for neoprene compared with 100 mol/m^3 for latex).
3. The faster VX permeation in latex was driven by the higher diffusivity value ($5 \times 10^{-12} \text{ m}^2/\text{s}$ for latex compared with $1.5 \times 10^{-12} \text{ m}^2/\text{s}$ for neoprene). This was also the reason that the breakthrough time is shorter for latex ($\sim 1.5 \text{ h}$) compared with neoprene ($\sim 7 \text{ h}$).

The LVAP model can provide additional insight for experiments and explain observations on the basis of the relative transport properties of materials and the sampler. In addition, it can enhance experimental design depending on the desired information. For example, if the goal was to confirm the breakthrough time, an LVAP experiment could be designed to vary the permeation times with the assumption that the VX in the sampler would transition over time from none to a quantifiable mass. With the model, these times can be more judiciously chosen to maximize the probability of determining a breakthrough time. Similarly, if the goal was to design an experiment to determine the threshold VX permeation time, the model would allow permeation times to be chosen in a more informed manner. Furthermore, modeling techniques enable the prediction of agent breakthrough time, which would require significant experimental sampling to determine otherwise.

3.2 Sensitivity Analysis

Physics-based modeling allows What-if? questions to be addressed quickly and cheaply as compared with relying solely on experimental methods. The effects of material thickness and transport properties are discussed in this section.

3.2.1 Effect of Material Thickness on Permeation

Material thicknesses can vary as a result of the manufacturing process or wear over time. It can be important to determine how permeation behavior changes with material thickness. The thickness values for latex and neoprene were varied $\pm 20\%$ from the nominal values used in the simulations described in Section 3.1, and the resulting permeation behaviors were compared as shown in Figure 6.

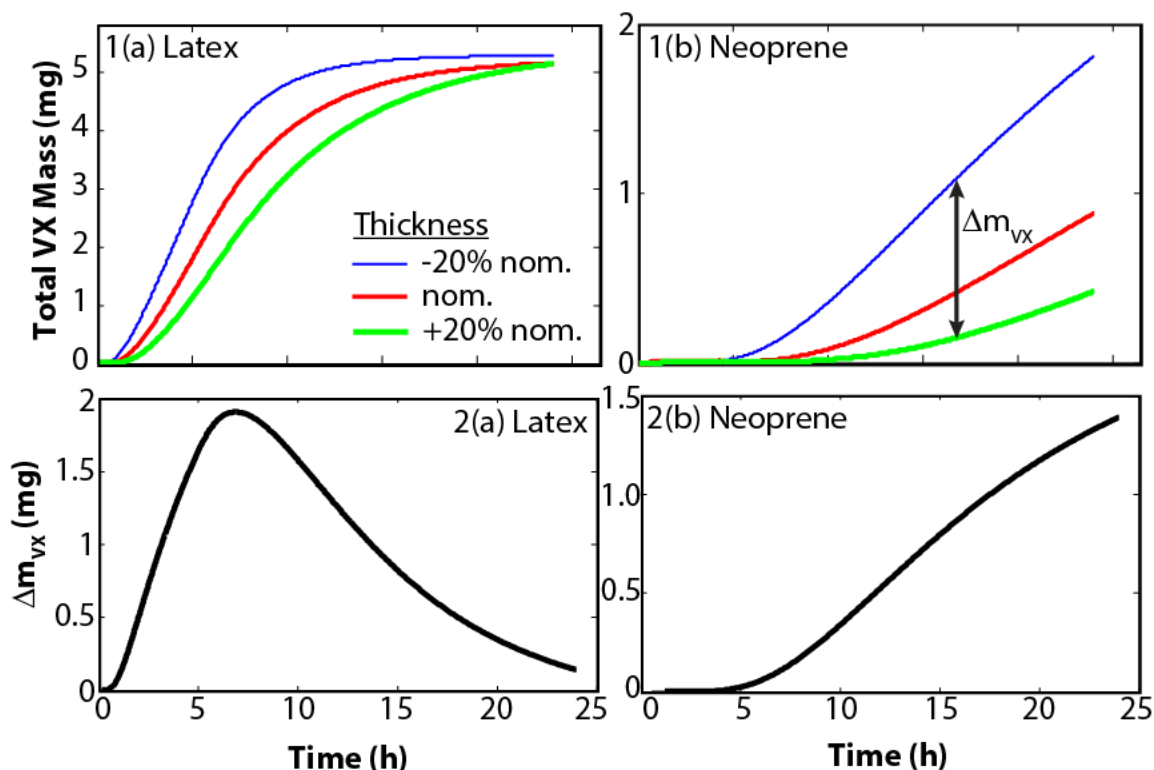


Figure 6. Model-predicted VX mass permeated through (1a) latex and (1b) neoprene as a function of time for nominal thicknesses and for +20 and –20% thicknesses. Also shown are the differences in permeated mass between the $\pm 20\%$ thickness extremes for both (2a) latex and (2b) neoprene.

Figure 6 clearly shows that thickness variation results in changes in agent mass permeation, and the difference in permeated mass, Δm_{vx} , changes throughout the experiment (i.e., as a function of time). The permeation curves for different thicknesses do not deviate before the breakthrough time. Because breakthrough occurs first for the thinner materials, this time marks where curve deviation begins. The latex permeation curves increase in deviation, reach a maximum deviation between 5 and 10 h, and then tend toward a common value as equilibrium is reached. The neoprene permeation curves monotonically increase in deviation with permeation time. However, the general trend that was observed for latex would be observed for neoprene if the experiment were run long enough to approach equilibrium. To summarize, reasonable material thickness variations can dramatically influence the agent mass permeated at a particular

time, but these differences tend to be minimized as equilibrium is approached. Modeling the system enables the prediction of the effect of this variable on experimental results.

3.2.2 Effect of Transport Properties on Permeation

The LVAP model can be used to investigate the effect of altering the transport properties on permeation behavior. In other words, hypothetical materials can be studied. All materials discussed in this section were modeled having an assumed material thickness of 500 μm . Although the model was developed under the assumption that agent transport occurs via Fickian diffusion, a reasonable approximation to a fabric (where capillary transport is usually the primary transport mechanism) was obtained by using relatively high values for $C_{\text{sat},m}$ and D_m . Figure 7 shows the permeation behavior in a simulated LVAP experiment using $C_{\text{sat},m} = 1000 \text{ mol/m}^3$ and $D_m = 1 \times 10^{-11} \text{ m}^2/\text{s}$ to approximate the permeation behavior of a porous material.

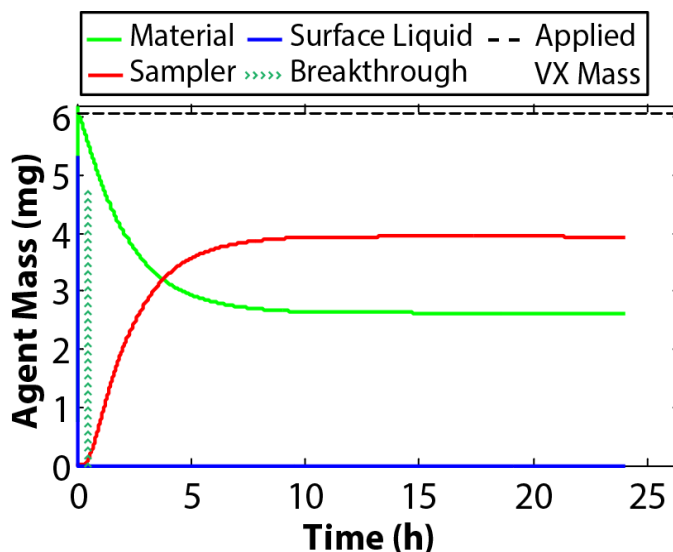


Figure 7. Model-predicted time evolution of agent mass in material and sampler throughout a simulated 24 h LVAP test for hypothetical porous material.

The liquid agent was quickly absorbed into the material, as would be expected because of the wicking process in a wetting porous material. Also, breakthrough occurred rapidly as compared with the latex and neoprene cases studied previously. Equilibrium occurred at around 10 h, when the agent mass in the material was retained, and no more agent permeated into the sampler. The equilibrium partitioning of agent was governed by the ratio of the solubilities in the material and sampler, $C_{\text{sat},m}$ and $C_{\text{sat},s}$, respectively. In Section 8, the possibility of expanding model capabilities to more accurately predict permeation in porous materials is discussed.

To approximate a polymeric material with low agent solubility, a lower value of $C_{\text{sat},m} = 10 \text{ mol/m}^3$ was used with $D_m = 1 \times 10^{-11} \text{ m}^2/\text{s}$, and the LVAP permeation results are shown in Figure 8.

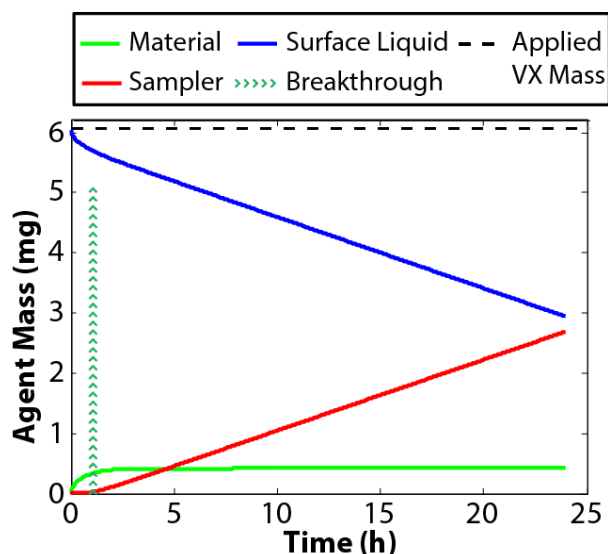


Figure 8. Model-predicted time evolution of agent mass in material and sampler throughout a simulated 24 h LVAP test for a hypothetical low-solubility material.

For the simulated LVAP test shown in Figure 8, the low solubility of agent in the material caused it to become saturated relatively quickly (within about 2 h). As agent permeated into the sampler, the diffusivity in the material was sufficiently large that the liquid agent on the surface continuously entered the material to keep it saturated. In this case, the permeation rate was limited by the solubility of the agent in the material. In this particular case, 24 h was insufficient to deplete the liquid from the surface, causing the amount of agent mass that permeated into the sampler to continue to increase at the end of the experiment.

The ideal material, from a purely personal protection perspective, would minimize agent solubility and diffusivity, although other design considerations could result in design tradeoffs. An example of an ideal barrier material was simulated by assuming $C_{\text{sat},m} = 10 \text{ mol/m}^3$ and $D_m = 1 \times 10^{-13} \text{ m}^2/\text{s}$. The permeation results shown in Figure 9 demonstrated that almost no agent permeation occurred over the course of 24 h, and that the liquid had not been depleted from the surface because of absorption into the material.

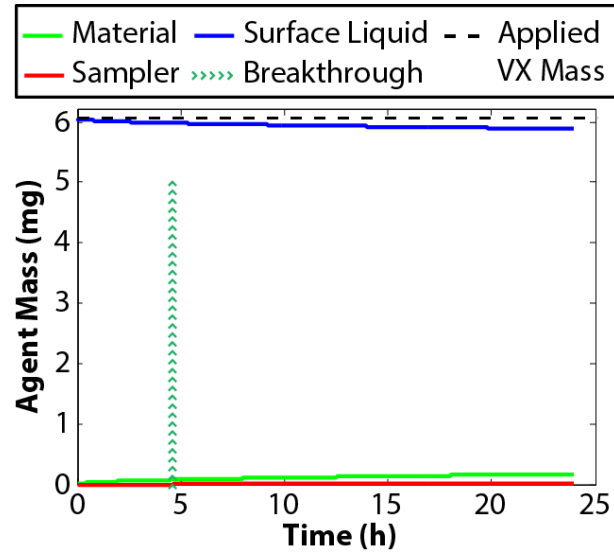


Figure 9. Model-predicted time evolution of agent mass in material and sampler throughout a simulated 24 h LVAP test for hypothetical barrier material.

4. COMPARISON OF LVAP AND AVLAG TEST METHODOLOGIES

The model of the AVLAG permeation test discussed in Section 2.2 was used to simulate the permeation of VX through latex and neoprene and to compare the results with those predicted for the LVAP model in Section 3.1. Whereas for the AVLAG model, six sessile 1 μL agent droplets were applied for the permeation test, another hypothetical case included modeled droplets that were uniformly spread into a 6 cm^2 area, which was similar to the thin film that forms when a weight is applied in the LVAP test. The VX mass that permeated through the material as a function of time in each of these simulated AVLAG tests was compared to the corresponding LVAP results for latex and neoprene in Figure 10.

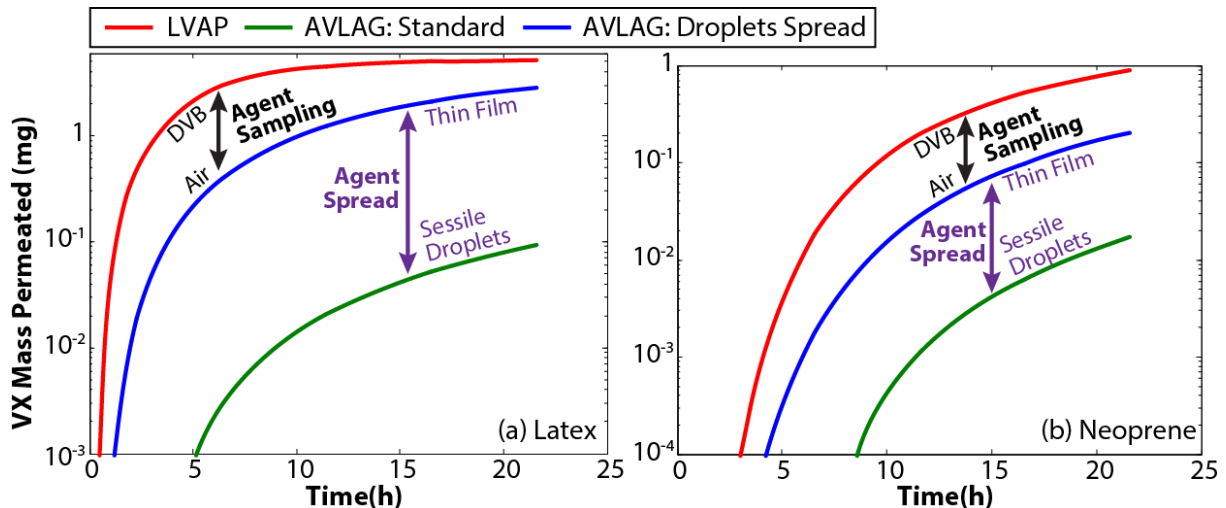


Figure 10. Comparison of VX mass permeated through (a) latex and (b) neoprene using the LVAP and AVLAG methods. Also shown are the results for a modified AVLAG method where the droplets were spread into a thin liquid film as opposed to being sessile.

The model results showed that the quantity of VX permeating through latex in the LVAP test was about 50 times greater than that in the standard AVLAG test, and it was about 5 times greater than the amount of VX permeating through neoprene after a 24 h period. The significantly lower amount of permeated agent mass observed in the AVLAG test was partially a function of the low vapor pressure of VX because it off-gasses from the material into the flowing air at a slow rate. The other factor influencing the difference in permeation rate between methods was the spreading of agent over a wider area on the material surface in the LVAP method. This is illustrated by examining the agent concentration distribution in a material during an AVLAG test as shown in Figure 11.

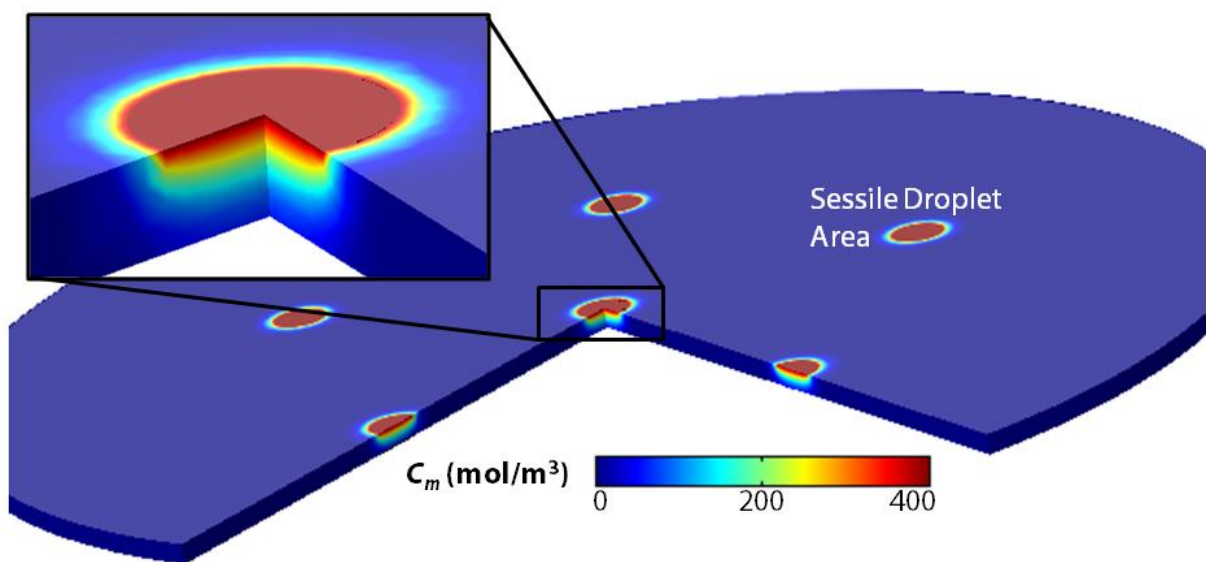


Figure 11. Contours of VX concentration during a simulated AVLAG cell test for VX permeation through neoprene.

If the liquid agent was uniformly spread in the form of a thin film, the permeation rate would increase over that of a droplet because of the increased contaminated area. This was confirmed by the model results shown in Figure 10, where the permeated agent mass in the AVLAG cell increased by a factor of approximately 25 for latex and by a factor of 5 for neoprene when the agent was spread uniformly instead of sitting as non-interacting sessile droplets on the material surface. This is a classic example of how modeling can be used to interpret test results and improve experimental designs. The model-predicted permeation results are summarized as a function of test method and agent spread in Table 3.

Table 3. Summary of Model-Predicted VX Permeation for Different Experimental Configurations

Test Method	Sampler	Agent Distribution	Mass Permeated (mg)	
			Latex	Neoprene
LVAP	Solid sorbent	Spread: thin film	5.2	0.95
AVLAG: standard	Flowing air	Sessile droplets	0.096	0.017
AVLAG: spread	Flowing air	Spread: thin film	2.9	0.23

The results presented in Figure 10 demonstrate the effects of droplet spread on permeated mass. This model-predicted result provides an example of how contaminant distribution affects the potential exposure of personnel. For example, if a latex glove were contaminated with six sessile droplets, the AVLAG tests were model-predicted to have a vapor breakthrough of 0.096 mg of VX after 22 h. However, if the same droplets were smeared on the latex glove (i.e., thin film) after handling by the

operator, the VX vapor breakthrough would be predicted to be 30 times greater. Modeling could be used to simulate permeation and resulting breakthrough for more or less droplets, different degrees of liquid agent spreading, and removal of agent at a specified time. Variations in these parameters may affect the exposure of personnel, and modeling enables a large number of scenarios to be investigated. These represent a few of the potential uses and What-if? types of questions that can be answered using modeling to determine the meaning and use of permeation data to address specific concerns related to operator exposure.

5. COMPARISON OF LVAP PERMEATION RESULTS TO IDEAL MODEL OF SKIN UPTAKE

A potentially useful application of the LVAP testing would be to predict the amount of agent uptake in a real-world operational situation in which the contaminated material would be worn in contact with a person's skin. Multiple practical details must be addressed to accurately perform this calculation, including the degree of material contact with the skin and how the material dynamically changes with motion and wear. The LVAP test model focuses on the worst-case scenario of perfect contact between material and skin, except that highly absorbent DVB is used to simulate the skin.

The model for agent transport through material and skin that are in perfect contact is equivalent to the model for the LVAP test (eqs 1–4) in which the skin layer is the sampler, except for the boundary condition that is enforced at the opposite side of the material–sampler interface. For the LVAP test, the sampler sits on an impermeable substrate; therefore, there is no flux of agent at this boundary. However, in the case of transport through skin, capillaries in the dermis absorb agent, and the blood flow carries it throughout the body. In the worst-case scenario, perfect absorption into the bloodstream is assumed, and the corresponding boundary condition, enforced on the opposite side of the material–skin interface, is an agent concentration of zero, which is used in the prediction.

This physics-based model can be used to predict agent permeation into any material, including skin. However, this requires knowledge of the transport parameters of agent in skin to accurately predict permeation behavior. Vallet et al. measured the steady-state permeability of VX through excised human abdominal skin in vitro using a diffusion cell technique. They found $K_p = 46.2 \times 10^{-6}$ cm/h (1.28×10^{-10} m/s).¹⁸ The permeability, K_p , is related to the partition coefficient of VX between its pure liquid phase and the stratum corneum (SC), $K_{SC/VX}$, and the diffusivity of VX in the SC, D_{SC} (eq 8).¹⁹

$$K_p = \frac{K_{SC/VX} D_{SC}}{S} \quad \text{Equation 8}$$

where

K_p is permeability of chemical through skin (m/s)

$K_{SC/VX}$ is partition coefficient of VX between SC and pure liquid phase (unitless)

D_{SC} is diffusivity of VX in SC (m²/s)

S is thickness of skin layer used in experiments (m)

Thus, it is generally not possible to find independent values for the partition coefficient and the diffusivity on the basis of permeability data alone. However, other experimental work that ascertained the octanol–water partition coefficient ($K_{o/w}$) of VX can be used to estimate the partition coefficient in eq 8, so that the diffusivity can be computed. Czerwinski et al. found that $\log_{10}(K_{o/w}) = 0.675$ for VX.²⁰ Because the solubility of VX in water is known to be approximately 112 mol/m^3 ,²¹ the solubility of VX in octanol is 530 mol/m^3 . If it is further assumed that the solubility in the lipid phase (subscript “lip”) is a factor of 1.25 higher than in octanol, as was done by Nitsche and Kasting,²² then $C_{\text{sat,VX,lip}} = 662 \text{ mol/m}^3$. However, because only about 10% of the SC consists of the lipid matrix, $C_{\text{sat,VX,SC}} = 66 \text{ mol/m}^3$. Knowing that the molar concentration of pure liquid VX is 3782 mol/m^3 , $K_{\text{SC/VX}} = 0.0175$, using eq 8 with $S = 1.75 \text{ mm}$ yields $D_{\text{SC}} = 1.25 \times 10^{-11} \text{ m}^2/\text{s}$. The approximate VX permeation through latex and neoprene, using these values for skin transport properties, was compared to VX permeation in a simulated LVAP experiment, as shown in Figure 12.

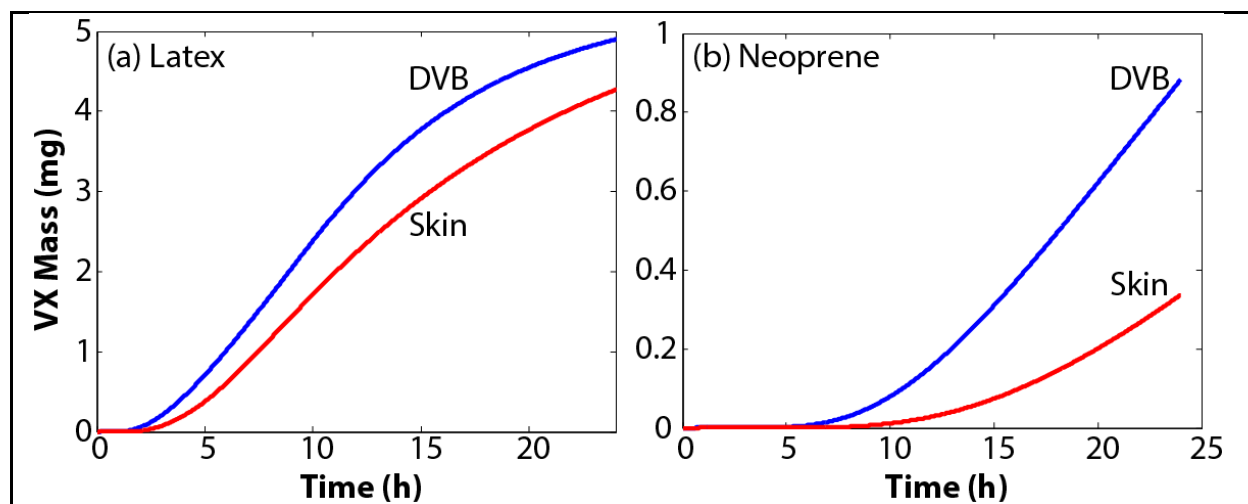


Figure 12. Mass of VX permeated through (a) latex and (b) neoprene in simulated LVAP tests using DVB and skin as samplers.

The results (Figure 12) show that DVB absorbs a similar amount of VX as compared to skin through both latex and neoprene. These results demonstrate that agent-permeation quantities obtained from LVAP experiments can produce useable worst-case estimates for real-world scenarios where the material is in direct contact with human skin. Conversely, Figure 10 and Table 3 show that the AVLAGE method provides significantly lower estimates for permeation through the test material and into the skin. The AVLAGE method corresponds to agent emitting as a vapor from the swatch material and producing a percutaneous exposure from the contaminant vapor, whereas the LVAP method provides an indication for direct skin transfer from the swatch. The combination of these techniques provides an upper and lower bound for exposures. The use of modeling demonstrates that the VX permeation process through the test material is similar for both methods, but the magnitude of the permeated mass measured is a function of the sampling media (air vs DVB) and contaminated area.

6. EFFECT OF VAPOR PRESSURE ON PERMEATION RATE IN AVLAGE CELL

The results discussed in Section 4 show that the low rate of agent permeation in an AVLAGE cell as compared with that of the LVAP test was partly due to the sampling method. In an AVLAGE cell, the permeant compound (i.e., the contaminant) is transferred from the test material swatch to flowing air; therefore, the agent permeation rate is partially controlled by the vapor pressure of the agent. For low vapor

pressure agents, the vapor emission process may be a rate-limiting step for the overall rate of agent permeation. On the other hand, in the LVAP method, a highly absorbent sampler is used to collect the agent permeating through the sample swatch so that the contaminant vapor pressure does not influence the permeation rate.

To demonstrate the effect of vapor pressure on experimental results, the permeation of a hypothetical agent, with a vapor pressure 10 times higher than VX, in an AVLAGE cell was simulated (with all other transport properties being equivalent to VX). In Figure 13, the mass of the hypothetical agent permeated after 24 h is higher than that of VX through both latex and neoprene by factors of approximately 5 and 3, respectively. These results demonstrated that, for AVLAGE measurements where all parameters were equal except vapor pressure, the quantity of permeated mass through a material is dependent on the vapor pressure of the contaminant. Because the LVAP test uses a solid-phase sampler in direct contact with the test material swatch, vapor pressure does not influence the permeated agent mass, and the model results are identical for the lower and higher vapor pressure agents.

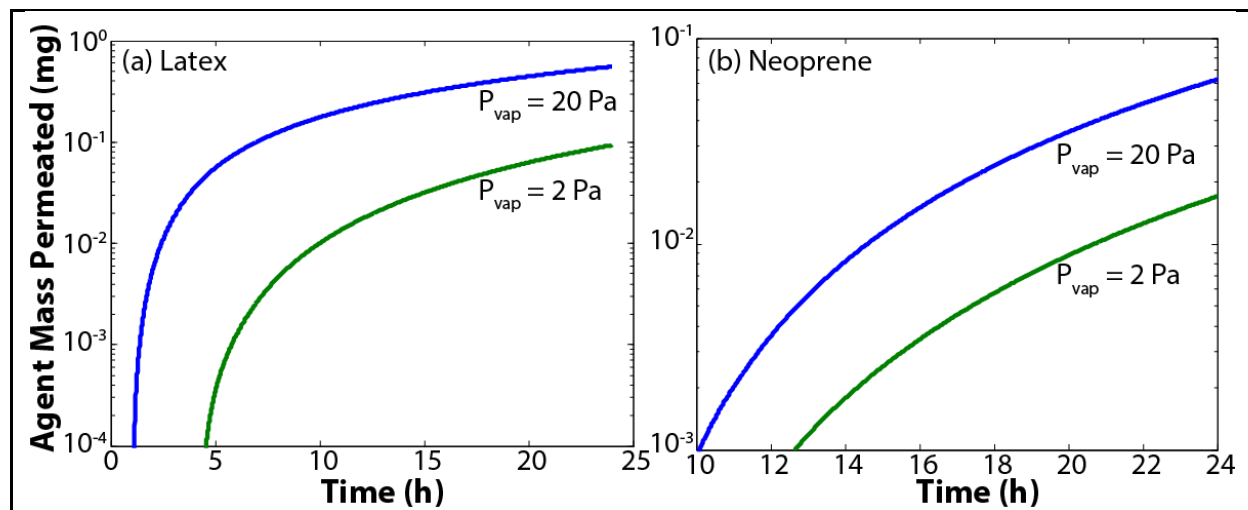


Figure 13. Comparison of predicted permeation results from simulated standard AVLAGE cell test using hypothetical agents with vapor pressures of 2 and 20 Pa for (a) latex and (b) neoprene.

For AVLAGE tests, the rate-limiting process could be either permeation through the material or emission into the vapor-collection air stream. However, in the LVAP test, uptake into the DVB sampler is so rapid that the rate-limiting process must be agent permeation through the material swatch. In both cases, the agent must permeate to the distal surface of the test material before it can be sampled by either air or DVB; therefore, the breakthrough time is similar for both techniques. However, the resulting magnitude and temporal trend of the agent permeation post-breakthrough is highly dependent upon the experimental technique used as well as on the contaminant and its physical properties (e.g., vapor pressure). As the vapor pressure of the agent increases (i.e., the transport resistance through the material becomes the dominant factor in determining permeation rate), the LVAP and AVLAGE tests should provide increasingly similar results. The use of lower vapor pressure agents (i.e., the transport resistance into the air stream becomes the dominant factor in determining permeation rate) will produce greater differences in results between the AVLAGE and LVAP tests.

These results demonstrate the operational interpretation of AVLAG and LVAP data. Coupling this information with agent transport properties of the skin (Section 5) enables estimation of percutaneous exposures from contaminant vapor. The LVAP test measures the agent that permeates through a material and into a highly absorbent sampler, which emulates direct contact of the skin with the material, and is applicable for direct agent transfer. In reality, when personal protective equipment materials are worn, the garment can have air gaps in places and come into direct contact with skin in other places. The combination of both techniques provides the opportunity for more-accurate exposure assessments. Combining AVLAG and LVAP modeling with similar experimental testing enables better interpretation of the differences between the techniques and helps to explain *why* different permeated mass values are observed.

If the purpose of the test is to determine when contaminant breakthrough occurs (i.e., how long a glove should be worn before replacement), the technique with the greater analytical sensitivity will provide the best indication. LVAP testing provides a measurement in which the transport resistance in the material determines the agent permeation rate, whereas AVLAG test results are dependent on the transport resistance in the material and in the contaminant vapor phase. Exclusively using experimental techniques to determine the breakthrough time makes it difficult to identify the threshold transition time at which analytically detectable agent mass would first occur. In addition, with a single time-point experiment like the LVAP test, multiple contact durations would have to be run and curve-fit to estimate the breakthrough time. Without any prior knowledge of the permeation behavior of the material, selecting contact times would be a trial-and-error process. However, with the implementation of modeling, the breakthrough time can be estimated so that time points can be more judiciously chosen, and the experimental results can, in turn, inform model accuracy.

The original purpose of the AVLAG test was to measure the breakthrough time and total mass breakthrough of contaminant for a material swatch over a given time.³ This was performed by quantifying the vapor emitted from the distal surface of a liquid-contaminated material. It was found that vapor detection of low-volatility contaminants was insufficient, and the total mass that had permeated was under-reported. This was the impetus behind developing the LVAP method. Through the modeling effort accomplished in this work, we have a better understanding of the physical processes that occur and how each contributes to the overall permeated contaminant mass. Additionally, the different methods provide information relevant to various real-world scenarios. The AVLAG test may be an appropriate method for low-volatility contaminants if there is an air gap and no direct contact will be made with the material. The LVAP test provides a more-appropriate estimate for a direct-contact scenario. As contaminant volatility increases, the transport dynamics become increasingly limited by the material phase, and it becomes less important what contacts the distal side of the material (i.e., skin, DVB, or air). In these cases, the AVLAG and LVAP tests are expected to provide more similar results.

7. EFFECTS OF IMPERFECT MATERIAL–SAMPLER CONTACT

The degree of contact between the material and sampler is an important consideration when evaluating LVAP test results. Experimental work shows that when no weight is applied to promote contact, the collected permeated agent mass is significantly less.⁴ Figure 14 shows an idealized view of imperfect contact at the material–sampler interface, where the material interface is approximated as a sinusoidal function, and the distance between the peak of a sine wave and the flat sampler interface, Δ , defines the contact area, A_c . As the value of Δ decreases, A_c increases, which should increase the agent permeation rate.

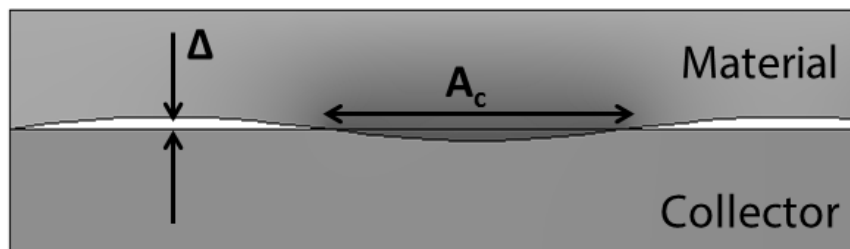


Figure 14. Schematic of model used to simulate imperfect contact between material and sampler during an LVAP test. A sinusoidal function is used to represent the surface of the material in contact with the sampler, and the distance (Δ) between the material and sampler controls the local contact area (A_c).

Figure 15 shows the permeated mass of VX through latex in a simulated LVAP experiment with varying degrees of contact. As expected, increasing the degree of contact caused an increase in permeation rate. This simplified view of the contact can also serve as the first step for a more-detailed study of variations in permeation for a real-world scenario in which personnel are wearing a garment or protective equipment that may not be in perfect contact with the user.

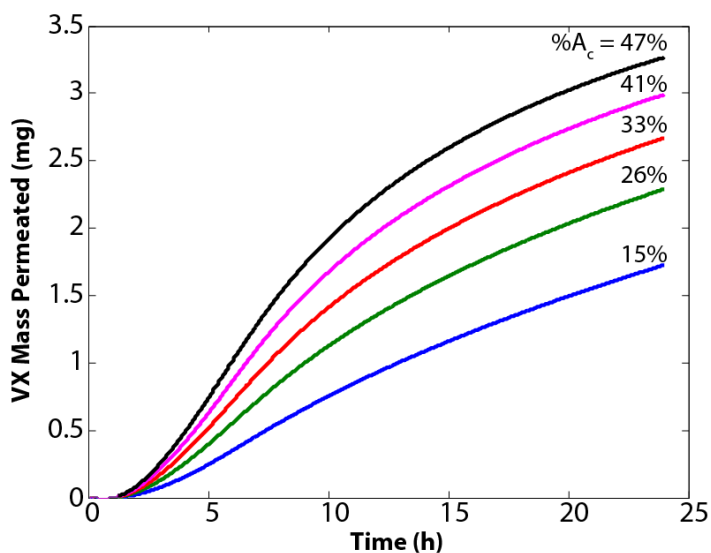


Figure 15. Mass of VX permeated through latex in an LVAP experiment with varying degrees of contact between the latex and DVB sampler.

8. CONCLUSIONS AND SUGGESTIONS FOR FUTURE WORK

Mathematical models were developed to predict agent permeation through materials in both LVAP and AVLAG tests. Model capabilities were demonstrated by comparing actual experimental results with model-predicted VX permeation through latex and neoprene in a simulated LVAP test. The model results provided additional insight beyond that gained by the experiments alone, including estimates of breakthrough time, depletion of liquid agent on the material surface, and possibilities for improved test design.

Permeation results equivalent to those from an actual AVLAG cell were simulated using the model. An analysis was performed to explain the differences in permeation rates between different experimental configurations. As a result, it was suggested that permeation rates in the AVLAG test could be increased by spreading liquid agent in a thin film to increase the contaminated area. The influence of material thickness, transport properties, and material–sampler contact were investigated to show how modeling can inform sensitivity of permeation to variations in critical parameters and to study hypothetical materials.

This work highlights the utility of modeling permeation for the specific case of inert polymeric materials. This type of study could be expanded by applying existing knowledge toward the development of modeling capabilities for agent permeation through more-complex materials such as fabrics, multilayer materials, and materials impregnated with active components (e.g., carbon for adsorption of agents). The models could then be used to optimize material design for particular performance metrics.

Another avenue for model application would be to critically evaluate permeation test methodologies to minimize the testing necessary to obtain the desired data, enhance the quality of data, and interpret the data more effectively. The work presented in this report provides examples of how modeling can be used to achieve these goals, specifically for LVAP and AVLAG test methodologies, and how modeling could be applied to evaluate larger-scale testing, different scenarios, and comparisons to health-based requirements. Lastly, modeling could be used to simulate contaminant exposure to personnel in probable environments and to estimate agent doses in various scenarios.

This report discussed several ways that LVAP and AVLAG modeling can support and strengthen permeation testing. Modeling will never replace testing, but it can be used to strengthen the test designs and interpretation of data, which can in turn accelerate testing and reduce costs. The application of physics-based models provides a fundamental understanding of the processes to enable the prediction of results and, ultimately, better control over the system. In this case, modeling also provided the link between toxicology and permeation testing, enabling the simulation of contaminant exposures to determine the potential doses delivered to personnel in many What-if? operational scenarios.

LITERATURE CITED

1. El Afif, A.; De Kee, D.; Cortez, R.; Gaver, D.P. Dynamics of Complex Interfaces. I. Rheology, Morphology, and Diffusion. *J. Chem. Phys.* **2003**, *118* (22), 10227–10243.
2. El Afif, A.; De Kee, D.; Cortez, R.; Gaver, D.P. Dynamics of Complex Interfaces. II. Diffusion and Morphology. *J. Chem. Phys.* **2003**, *118* (22), 10244–10253.
3. *Test Operations Procedure (TOP) 8-2-501A, Permeation and Penetration of Air-Permeable, Semipermeable, and Impermeable Materials with Chemical Agents or Simulants (Swatch Testing)*; TOP 8-2-501A; West Desert Test Center: Dugway Proving Ground, UT, 08 May 2013. UNCLASSIFIED Report.
4. D’Onofrio, T.G. *Development of a Contact Permeation Test Fixture and Method*; ECBC-TR-1141; U.S. Army Edgewood Chemical Biological Center: Aberdeen Proving Ground, MD, 2013. UNCLASSIFIED Report.
5. Hines, A.L.; Maddox, R.N. *Mass Transfer: Fundamentals and Applications*; Prentice Hall: Englewood Cliffs, NJ, 1985.
6. Vieth, W.R. *Diffusion In and Through Polymers: Principles and Applications*, 1st ed.; Hanser: Barcelona, 1991.
7. Crank, J. *The Mathematics of Diffusion*. Oxford University Press: New York, 1980; 424.
8. Koros, W.J.; Madden, W. Transport Properties. In *Encyclopedia of Polymer Science and Technology*; Mark, H.F., Kroschwitz, J.I., Eds.; Vol. 12; John Wiley & Sons: Hoboken, NJ, 2004; 291–381.
9. Incropera, F.P.; Dewitt, D.P.; Bergman, T.L.; Lavine, A.S. *Fundamentals of Heat and Mass Transfer*, 6th ed.; John Wiley & Sons: Hoboken, NJ, 2007.
10. Willis, M.P.; Mantooth, B.A.; Lalain, T. Novel Methodology for the Estimation of Chemical Warfare Agent Mass Transport Dynamics, Part I: Evaporation. *J. Phys. Chem. C* **2011**, *116* (1), 538–545.
11. Willis, M.P.; Mantooth, B.A.; Lalain, T. Novel Methodology for the Estimation of Chemical Warfare Agent Mass Transport Dynamics, Part II: Absorption. *J. Phys. Chem. C* **2011**, *116* (1), 546–554.
12. D’Onofrio, T.G.; Davies, J.P.; Steinbach, C.B.; Ruppert, C.J. *Low-Volatility Agent Permeation (LVAP) Verification and Validation Report*; ECBC-TR-1274; U.S. Army Edgewood Chemical Biological Center: Aberdeen Proving Ground, MD, 2015. UNCLASSIFIED Report.
13. Harogopad, S.B.; Aminabhavi, T.M. Diffusion and Sorption of Organic Liquids through Polymer Membranes .5. Neoprene–Styrene–Butadiene–Rubber, Ethylene–Propylene–Diene Terpolymer, and Natural Rubber Versus Hydrocarbons (C₈–C₁₆). *Macromolecules* **1991**, *24* (9), 2598–2605.

14. Harogopad, S.B.; Aminabhavi, T.M. Diffusion and Sorption of Organic Liquids through Polymer Membranes 2. Neoprene, SBR, EPDM, NBR, and Natural Rubber versus *n*-Alkanes. *J. Appl. Polym. Sci.* **1991**, *42* (8), 2329–2336.
15. Buchanan, J.H.; Buettner, L.C.; Butrow, A.B.; Tevault, D.E. *Vapor Pressure of VX*; ECBC-TR-068; U.S. Army Edgewood Chemical Biological Center: Aberdeen Proving Ground, MD, 1999. UNCLASSIFIED Report.
16. Perry, R.H.; Green, D.W. *Perry's Chemical Engineer's Handbook*, 7th ed.; Perry, R.H., Green, D.W., Eds.; McGraw-Hill Professional: New York, 1997.
17. *COMSOL Multiphysics User's Guide*, 4.3b; Comsol, Inc.: Stockholm, Sweden, 2013.
18. Vallet, V.; Cruz, C.; Licausi, J.; Bazire, A.; Lallement, G.; Boudry, I. Percutaneous Penetration and Distribution of VX Using In Vitro Pig or Human Excised Skin Validation Of Demeton-S-Methyl as Adequate Simulant for VX Skin Permeation Investigations. *Toxicology* **2008**, *246* (1), 73–82.
19. Fitzpatrick, D.; Corish, J.; Hayes, B. Modelling Skin Permeability in Risk Assessment—The Future. *Chemosphere* **2004**, *55* (10), 1309–1314.
20. Czerwinski, S.; Skvorak, J.; Maxwell, D.; Lenz, D.; Baskin, S. Effect of Octanol:Water Partition Coefficients of Organophosphorus Compounds on Biodistribution and Percutaneous Toxicity. *J. Biochem. Mol. Toxicol.* **2006**, *20* (5), 241–246.
21. Bizzigotti, G.O.; Castelly, H.; Hafez, A.M.; Smith, W.H.B.; Whitmire, M.T. Parameters for Evaluation of the Fate, Transport, and Environmental Impacts of Chemical Agents in Marine Environments. *Chem. Rev.* **2009**, *109* (1), 236–256.
22. Nitsche, J.M.; Kasting, G.B. A Microscopic Multiphase Diffusion Model of Viable Epidermis Permeability. *Biophys. J.* **2013**, *104*, 2307–2320.

ACRONYMS AND ABBREVIATIONS

AVLAG	Aerosol Vapor Liquid Assessment Group
DCA	dynamic contact angle
DUSA TE	Deputy Under Secretary of the Army for Test and Evaluation
DVB	divinyl benzene
LVAP	low-volatility agent permeation
MW	molecular weight
SC	stratum corneum
VX	<i>O</i> -ethyl- <i>S</i> -(2-isopropylaminoethyl) methylphosphonothiolate, persistent nerve agent

DISTRIBUTION LIST

The following individuals and organizations were provided with one Adobe portable document format (pdf) electronic version of this report:

ECBC Decontamination Sciences Branch
RCDB-DRP-D
Attn: Mantooth, B.

G-3 History Office
U.S. Army RDECOM
Attn: Smart, J.

ECBC Decontamination Sciences Branch
RCDB-DRP-D
Attn: Shue, M.

ECBC Technical Library
RDCB-DRB-BL
Attn: Foppiano, S.
Stein, J.

Defense Threat Reduction Agency
DTRA/RD-CBD T
Attn: Ward, T.
J9-CBS
Attn: Moore, E.

Office of the Chief Counsel
AMSRD-CC
Attn: Upchurch, V.

Department of Homeland Security
DHS ORD CSAC
Attn: Famini, G.

Defense Technical Information Center
Attn: DTIC OA

ECBC Rock Island
RDCB-DES
Attn: Lee, K.

